

# Thermodynamic Characterization of Ligand-Induced Conformational Changes in UDP-*N*-acetylglucosamine Enolpyruvyl Transferase<sup>†</sup>

Anne K. Samland,<sup>‡</sup> Ilian Jelesarov,<sup>§</sup> Roger Kuhn,<sup>‡</sup> Nikolaus Amrhein,<sup>‡</sup> and Peter Macheroux<sup>\*,‡</sup>

*Institut für Pflanzenwissenschaften, Eidgenössische Technische Hochschule Zürich, Universitätstrasse 2, CH-8092 Zürich, Switzerland, and Institut für Biochemie, Universität Zürich, Winterthurerstrasse 190, CH-8057 Zürich, Switzerland*

Received April 6, 2001; Revised Manuscript Received June 27, 2001

**ABSTRACT:** The binding of UDP-*N*-acetylglucosamine (UDPNAG) to the enzyme UDP-*N*-acetylglucosamine enolpyruvyl transferase (MurA) was studied in the absence and presence of the antibiotic fosfomycin by isothermal titration calorimetry. Fosfomycin binds covalently to MurA in the presence of UDPNAG and also in its absence as demonstrated by MALDI mass spectrometry. The covalent attachment of fosfomycin affects the thermodynamic parameters of UDPNAG binding significantly: In the absence of fosfomycin the binding of UDPNAG is enthalpically driven ( $\Delta H = -35.5 \text{ kJ mol}^{-1}$  at 15 °C) and opposed by an unfavorable entropy change ( $\Delta S = -25 \text{ J mol}^{-1} \text{ K}^{-1}$ ). In the presence of covalently attached fosfomycin the binding of UDPNAG is entropically driven ( $\Delta S = 187 \text{ J mol}^{-1} \text{ K}^{-1}$  at 15 °C) and associated with unfavorable changes in enthalpy ( $\Delta H = 28.8 \text{ kJ mol}^{-1}$ ). Heat capacities for UDPNAG binding in the absence or presence of fosfomycin were  $-1.87$  and  $-2.74 \text{ kJ mol}^{-1} \text{ K}^{-1}$ , respectively, indicating that most ( $\approx 70\%$ ) of the conformational changes take place upon formation of the UDPNAG–MurA binary complex. The major contribution to the heat capacity of ligand binding is thought to be due to changes in the solvent-accessible surface area. However, associated conformational changes, if any, also contribute to the experimentally measured magnitude of the heat capacity. The changes in solvent-accessible surface area were calculated from available 3D structures, yielding a  $\Delta C_p$  of  $-1.3 \text{ kJ mol}^{-1} \text{ K}^{-1}$ ; i.e., the experimentally determined heat capacity exceeds the calculated one. This implies that other thermodynamic factors exert a large influence on the heat capacity of protein–ligand interactions.

The first step in peptidoglycan biosynthesis in most eubacteria is catalyzed by the enzyme UDP-*N*-acetylglucosamine enolpyruvyl transferase (MurA)<sup>1</sup> which catalyzes the transfer of the intact enolpyruvyl moiety from phosphoenolpyruvate (PEP) to the 3'-hydroxyl group of UDP-*N*-acetylglucosamine (UDPNAG) (Scheme 1A) (1). A second enzyme known to catalyze a similar reaction is 5-enolpyruvylshikimate 3-phosphate (EPSP) synthase, the sixth enzyme of the shikimate pathway which is the biosynthetic pathway of the aromatic amino acids and their derivatives in plants, microbes, fungi, and apicomplexa (2, 3). EPSP synthase transfers the enolpyruvyl residue from PEP to the 5-hydroxyl group of shikimate 3-phosphate with the concomitant release

of inorganic phosphate. Recently, a third enzyme (NikO) which shows significant sequence similarity to MurA and EPSP synthase was discovered from *Streptomyces tendae* and is presumed to catalyze a similar reaction in the biosynthetic pathway of the antibiotic nikkomycin (4). As the pathway of peptidoglycan biosynthesis is restricted to eubacteria and the shikimate pathway to microorganisms and plants, these enzymes are important potential targets for the development of new antibiotics and herbicides. Despite their structural and mechanistic similarities, inhibitors of these enzymes show a high specificity. Glyphosate, the active ingredient in the broad spectrum and widely used herbicide Roundup, specifically inhibits EPSP synthase, while the antibiotic fosfomycin acts only on MurA by binding covalently to the catalytically important cysteine 115 (Scheme 1B). For a more comprehensive understanding of the action of an inhibitor as well as for the design of new inhibitors, a structural and thermodynamic characterization of the binding of the inhibitor to the protein and the processes associated with it is desirable.

In the last 5 years several 3D structures of MurA have become available; the unliganded enzyme is represented as an open conformation (see Figure 1, left structure) (5), the three-dimensional topology of which is similar to that of unliganded EPSP synthase (6). Interestingly, both enzymes consist of two globular domains with an unique "inside-out  $\alpha/\beta$ -barrel" fold connected by a hinge region (5, 6).

<sup>†</sup> This work was supported by the ETH through an internal research grant to P.M. and N.A. (0-20-515-98).

\* To whom correspondence should be addressed. Tel: +41-1-6327827. Fax: +41-1-6321044. E-mail: peter.macheroux@ipw.biol.ethz.ch.

<sup>‡</sup> Eidgenössische Technische Hochschule Zürich.

<sup>§</sup> Universität Zürich.

<sup>1</sup> Abbreviations: ANS, 8-anilino-1-naphthalenesulfonate; CD, circular dichroism; EPSP, 5-enolpyruvylshikimate 3-phosphate; fosfomycin (FF), (1R,2S)-1,2-epoxypropylphosphonic acid; glyphosate, *N*-(phosphonomethyl)glycine; HEPES, 4-(2-hydroxyethyl)piperazine-1-ethanesulfonic acid; ITC, isothermal titration calorimetry; MurA, UDP-*N*-acetylglucosamine enolpyruvyl transferase; PEP, phosphoenolpyruvate; PIPES, piperazine-1,4-bis(2-ethanesulfonic acid); S3P, shikimate 3-phosphate; Tris, tris(hydroxymethyl)aminomethane; UDPNAG, UDP-*N*-acetylglucosamine;  $\Delta C_p$ , heat capacity change;  $\Delta G$ , free energy change;  $\Delta H$ , enthalpy change;  $\Delta S$ , entropy change.

Scheme 1

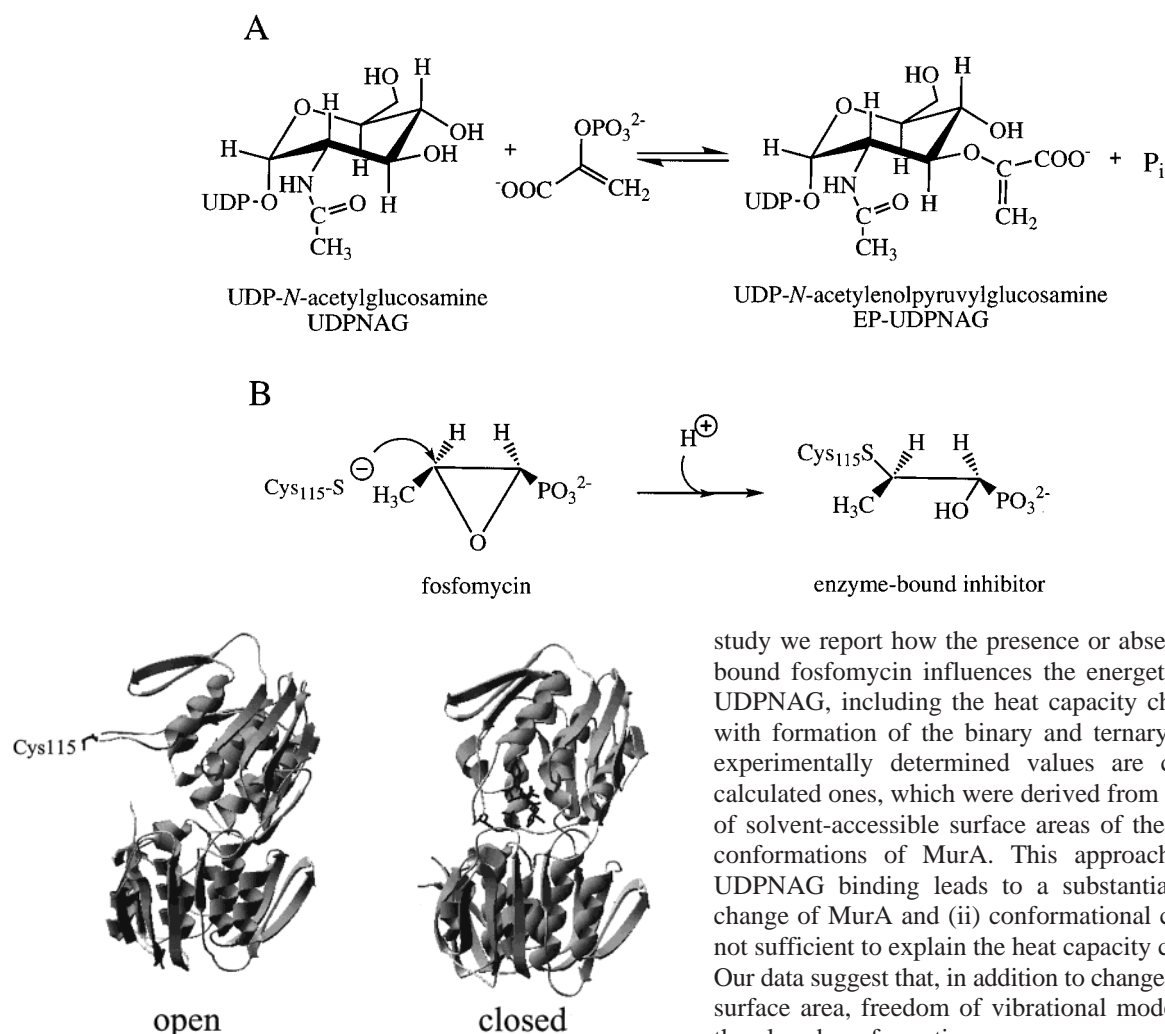


FIGURE 1: Structure of MurA in the open [PDB entry 1NAW (5)] and closed [PDB entry 1UAE (7)] conformations. The catalytically important residue C115 is highlighted. The closed conformation shows MurA cocrystallized with UDPNAG and fosfomycin.

Moreover, the structurally and mechanistically important loop of MurA between prolines 112 and 121 containing the catalytically essential cysteine 115 is solvent exposed. On the other hand, the structure of MurA complexed with either UDPNAG and fosfomycin (see Figure 1, right structure) (7) or the fluoro analogue of the tetrahedral reaction intermediate (MurA, UDPNAG, FPEP) (8) reflects a closed conformation. Therefore, it has been concluded that ligand binding is associated with a conformational change which involves the two domains moving toward each other with the loop closing the active site formed in the cleft between the domains (9). Further investigations of UDPNAG binding to MurA by small-angle X-ray scattering and binding studies using 8-anilino-1-naphthalenesulfonate (ANS) as an extrinsic fluorophore suggested a partial conformational change upon UDPNAG binding (10). This was also concluded from limited proteolysis experiments with MurA, which revealed a protective effect of UDPNAG (11).

To obtain more quantitative information on the process of UDPNAG binding and the associated conformational change, we investigated the binding of UDPNAG and fosfomycin by isothermal titration calorimetry. In the present

study we report how the presence or absence of covalently bound fosfomycin influences the energetics of binding of UDPNAG, including the heat capacity changes associated with formation of the binary and ternary complexes. The experimentally determined values are compared to the calculated ones, which were derived from the determination of solvent-accessible surface areas of the open and closed conformations of MurA. This approach shows that (i) UDPNAG binding leads to a substantial conformational change of MurA and (ii) conformational changes alone are not sufficient to explain the heat capacity changes observed. Our data suggest that, in addition to changes of the accessible surface area, freedom of vibrational modes is restricted in the closed conformation.

## MATERIALS AND METHODS

**Chemicals and Enzymes.** Fosfomycin and UDP-*N*-acetylglucosamine (sodium salt) were from Sigma, Buchs, Switzerland. 1,4-Dithio-DL-threitol, ethylenediaminetetraacetic acid (EDTA), isopropyl  $\beta$ -D-1-thiogalactopyranoside, HEPES, and PIPES were from Fluka, Buchs, Switzerland. Tris was from BDH Laboratory Supplies, Poole, England.

Trypsin (EC 3.4.21.4) from bovine pancreas (12 081 units/mg; chymotrypsin activity  $\leq 0.2\%$ ) was from Fluka, Buchs, Switzerland.

**Expression and Purification of the Protein.** Wild-type MurA from *Enterobacter cloacae* was expressed and purified as described previously (12). The protein concentration was determined using an extinction coefficient of 24 020 M<sup>-1</sup> cm<sup>-1</sup> at 280 nm.

**Isothermal Titration Calorimetry.** For determination of the heat capacity, all measurements were carried out in 50 mM HEPES/NaOH, pH 7.4, containing 2 mM DTT and 0.5 mM EDTA. Sample preparation and titrations were performed as described previously using a Omega titration calorimeter from Microcal, Inc. (13). For the binding of UDPNAG to free MurA, a solution of 200  $\mu$ M MurA was titrated with 5 mM UDPNAG at the indicated temperature, whereas in the case of UDPNAG binding to MurA covalently bound to

fosfomycin, MurA (190  $\mu$ M) was preincubated with 42 mM fosfomycin and titrated with 5 mM UDPNAG.

To determine heat contributions due to coupled protonation events upon binding, these two titrations were repeated in various buffers of different ionization enthalpies under otherwise identical conditions. The buffers and their ionization enthalpies (in kilojoules per mole at 15 °C) were as follows: PIPES (11.26), HEPES (20.5), and Tris (47.9) (14). For Tris buffer the ionization enthalpy of 47.4 kJ mol<sup>-1</sup> at 25 °C (15) was extrapolated to 15 °C with the heat capacity of Tricine (14). The pH of the buffer was adjusted at the experimental temperature. The buffer concentration was 50 mM.

**MALDI-TOF-MS Analysis of Fosfomycin Binding.** MurA (100  $\mu$ M) was incubated with 25 mM fosfomycin in 50 mM Tris-HCl, pH 7.4, for 30 min at 25 °C. The tryptic digest and MALDI-TOF analysis were performed as reported recently (16). To remove unbound fosfomycin prior to digestion, the samples were purified on a PD-10 column (Amersham Pharmacia Biotech) as described previously (17).

**Calculation of Solvent-Accessible Surface Area.** Solvent-accessible surface areas of MurA in its closed and open conformations were calculated using the program NACCESS (18) and the PDB files of the 3D structural data deposited in the database (Table 2). As there are two monomers of MurA present in the asymmetric cell of the crystals of unliganded MurA, the accessible surface areas were calculated for both monomers, and the average was used for further calculations. A probe size of 1.4 Å was used. From these data the changes in polar and apolar solvent-accessible surface area were calculated (Table 3). The polar and apolar contributions to the total change in accessible surface were then used to calculate the heat capacity for the binding processes, according to

$$\Delta C_p = \Delta c_{ap} \Delta ASA_{ap} - \Delta c_{pol} \Delta ASA_{pol} \quad (1)$$

where  $\Delta ASA$  is the apolar (ap) and polar (pol) surface buried in the complex and  $\Delta c$  is the elementary contribution per squared angstrom of apolar and polar surface in the heat capacity change (19). Since the structures of the open and closed forms of MurA were solved with the enzymes from *En. cloacae* and *Escherichia coli*, respectively, it is important to note that the sequence identity of these proteins is 93.6% with the majority of exchanges being conservative in nature.

## RESULTS

The binding of UDPNAG to MurA and the binding of fosfomycin to the binary complex of MurA and UDPNAG are amenable to microcalorimetry as the binding processes are associated with observable heat changes (13). In this study we extended previous studies with the aim to investigate conformational changes associated with ligand binding to MurA.

**Binding of UDPNAG and Fosfomycin.** As previously noted, fosfomycin binds preferentially to the binary complex of MurA and UDPNAG (9, 20). In the presence of UDPNAG inhibition kinetics revealed a dissociation constant of 8.6  $\mu$ M for the initial (i.e., noncovalent) ternary fosfomycin–UDPNAG–MurA complex (20). Using tryptophan fluorescence, addition of fosfomycin to MurA resulted in a

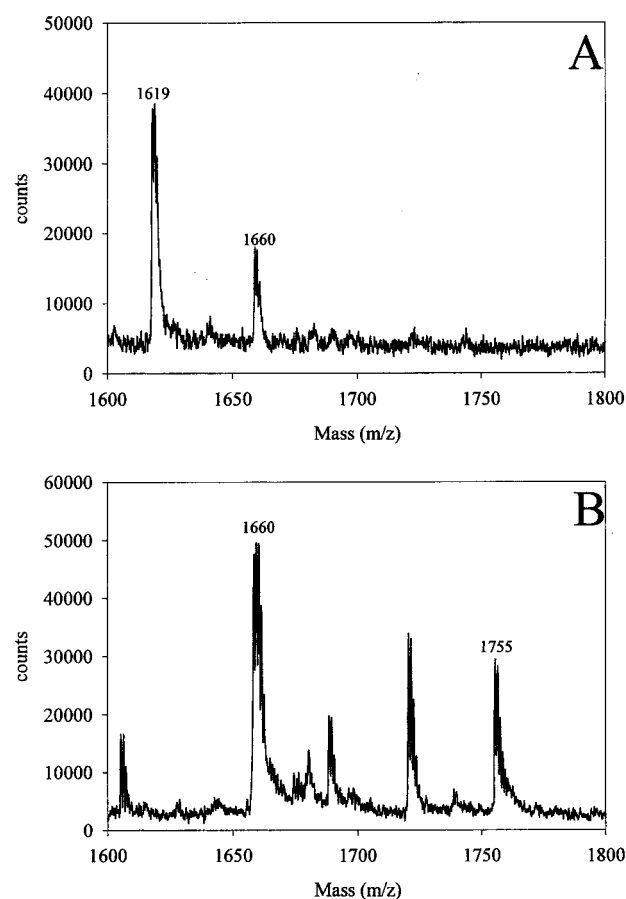


FIGURE 2: Mass spectral analysis of free MurA (panel A) and MurA preincubated with high fosfomycin concentrations (panel B). The mass peak at 1619 is due to the fragment comprising amino acids 104–120 and disappears upon formation of the covalent adduct with fosfomycin creating a new peak at 1755.

Table 1: Thermodynamic Parameters for the Binding of UDPNAG to Free MurA or MurA Covalently Bound to Fosfomycin<sup>a</sup>

T (°C)	MurA + UDPNAG			MurA-FF + UDPNAG		
	$\Delta H$	$\Delta G$	$T\Delta S$	$\Delta H$	$\Delta G$	$T\Delta S$
15	-35.5	-27.6	-7.2	28.8	-25.1	53.0
20	-46.8	-25.5	-21.4	12.9	-27.0	39.8
25	-52.8	-24.5	-28.3	≈0		
30	-64.6	-23.8	-40.9	-12.5	-27.1	14.5
$\Delta C_p$	-1.87			-2.74		

<sup>a</sup> All measurements were performed in 50 mM HEPES, pH 7.4. Values are means of duplicate experiments. Values of  $\Delta G$ ,  $\Delta H$ , and  $T\Delta S$  are in kJ mol<sup>-1</sup>;  $\Delta C_p$  is in kJ mol<sup>-1</sup> K<sup>-1</sup>.  $\Delta G$  was calculated from  $\Delta G = -RT \ln K_B$ , where  $K_B$  is the binding constant determined by ITC. The errors are estimated to be  $\pm 1\%$  for  $\Delta G$ ,  $\pm 3\%$  for  $\Delta H$ ,  $\pm 9\%$  for  $\Delta S$ , and 15% for  $\Delta C_p$ .

fluorescence quenching (data not shown) indicating that fosfomycin binding occurs in the absence of UDPNAG, albeit with a lower avidity. Further analysis by MALDI-TOF mass spectroscopy revealed that fosfomycin, even in the absence of UDPNAG, is covalently linked to C115 (see Figure 2). As unbound fosfomycin was removed prior to the tryptic digest, it can be excluded that fosfomycin had reacted with the digested peptides.

The covalent binding of fosfomycin to C115 of MurA also affects the thermodynamic parameters of UDPNAG binding (see Table 1 and Scheme 2). Therefore, calorimetric studies of UDPNAG binding to MurA alone and in the presence of

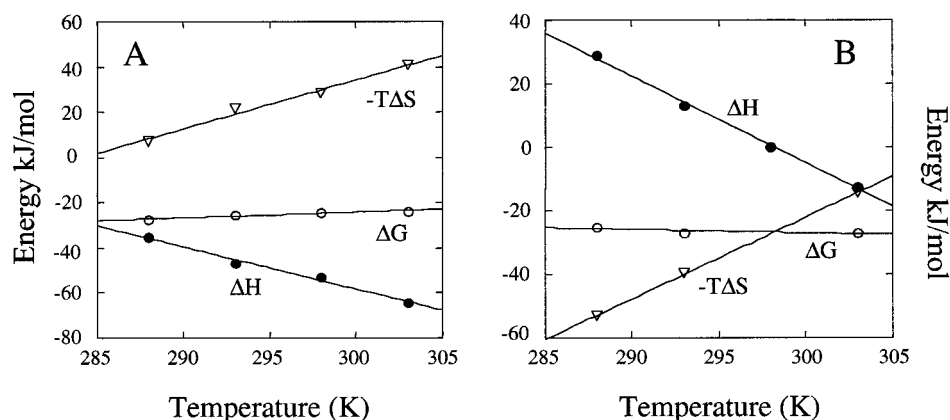
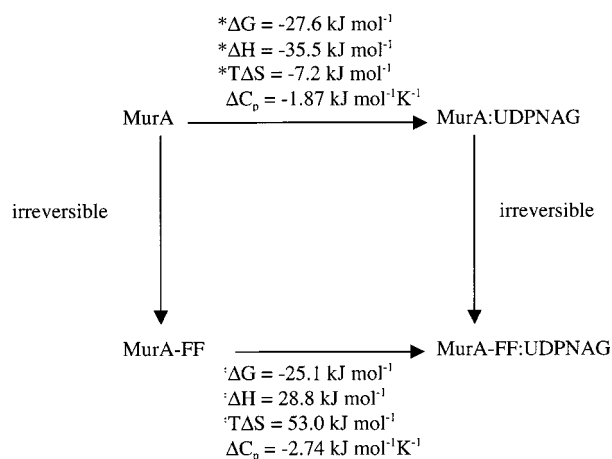


FIGURE 3: Temperature dependence of  $\Delta H$  (full circles),  $-T\Delta S$  (open triangles), and  $\Delta G$  (open circles) for the binding of UDPNAG to MurA (panel A) and for binding of UDPNAG to MurA–fosfomycin (panel B). ITC experiments were performed in 50 mM HEPES, pH 7.4, containing 2 mM DTT and 0.5 mM EDTA. MurA (190  $\mu$ M) alone or preincubated with 42 mM fosfomycin was titrated with 5 mM UDPNAG.  $\Delta C_p$  was obtained by the slope of a linear regression to the  $\Delta H$  data.

Scheme 2<sup>a</sup>



<sup>a</sup> Values indicated with an asterisk were measured at 15 °C.

high fosfomycin concentrations sufficient to generate the covalent MurA adduct were carried out.

**Temperature Dependence of Thermodynamic Parameters.** To determine the heat capacity associated with the binding processes, ITC experiments were performed at 15, 20, 25, and 30 °C. The results are presented in Figure 3 and summarized in Table 1. The binding of UDPNAG to free MurA is enthalpically driven with a large negative enthalpy and an unfavorable entropy change, whereas the binding to the binary complex (MurA–fosfomycin) is endothermic and entropically favored. At 25 °C, this reaction is not accompanied by any measurable heat change and is only entropically driven.  $\Delta H$  and  $T\Delta S$  depend strongly on the temperature, while  $\Delta G$  is almost insensitive to temperature due to enthalpy–entropy compensation. The heat capacity  $\Delta C_p$  was calculated from the slope of the regression lines of  $\Delta H$  versus temperature. The binding of UDPNAG to MurA in the absence and presence of fosfomycin was characterized by  $\Delta C_p = -1.87 \text{ kJ mol}^{-1} \text{K}^{-1}$  and  $\Delta C_p = -2.74 \text{ kJ mol}^{-1} \text{K}^{-1}$ , respectively (see Table 1 and Scheme 2).

**Correlation between  $\Delta C_p$  and Surface Area Buried on Substrate Binding.** Thermodynamic parameters for ligand–protein interaction can be related to changes in solvent-accessible surface area. With the structures of the open and closed conformations available, the changes of solvent-accessible surface area (see Table 2) could be determined,

Table 2: Accessible Surface of Liganded and Unliganded Forms of MurA and the Ligands<sup>a</sup>

structure	PDB entry	total surface (Å <sup>2</sup> )	polar surface (Å <sup>2</sup> )	apolar surface (Å <sup>2</sup> )
open conformation of wild-type MurA from <i>En. cloacae</i>	1NAW			
chain a		15 974	7213	8761
chain b		15 827	7161	8666
average of a and b chains		15 901	7187	8714
open conformation of C115S MurA from <i>En. cloacae</i>	1DLG			
chain a		16 403	7487	8917
chain b		16 492	7586	8907
average of a and b chains		16 445	7536	8912
closed conformation of wild-type MurA ( <i>E. coli</i> ) with UDPNAG and fosfomycin	1UAE	14 869	6950	7919
closed conformation of C115A mutant MurA ( <i>E. coli</i> ) with UDPNAG and FPEP	1A2N	14 982	7076	7905
UDPNAG		722	432	290
FPEP		843	538	305
fosfomycin		263	145	118

<sup>a</sup> The errors are assumed to be  $\pm 10\%$  for the calculated surface areas.

and from this the expected changes in heat capacity (see Table 3) were calculated as described in Materials and Methods. The  $\Delta ASA$  and  $\Delta C_p$  values calculated for various combinations of conformational changes from the open conformation of either wild-type or the C115S mutant protein to the closed conformation of different complexes, cocrystallized with either UDPNAG and fosfomycin or a fluoro analogue of the tetrahedral reaction intermediate, are summarized in Table 3. The buried apolar surface area is larger than the buried polar surface area. The calculated heat capacity change for the entire process (Table 3), from the free enzyme to the ternary complex ( $\Delta C_p = -1.3 \text{ kJ mol}^{-1} \text{K}^{-1}$ ), is significantly smaller than the experimentally determined heat capacities for the partial processes (Table 1).

**Determination of Protonation Enthalpies.** Substrate binding and conformational changes associated with it can influence the environment of some amino acids and, hence,



Table 3: Changes in Solvent-Accessible Surface Areas<sup>a</sup>

binding event	$\Delta\text{ASA}_{\text{total}}$ (Å <sup>2</sup> )	$\Delta\text{ASA}_{\text{pol}}$ (Å <sup>2</sup> )	$\Delta\text{ASA}_{\text{ap}}$ (Å <sup>2</sup> )	$\Delta C_p$ (kJ mol <sup>-1</sup> K <sup>-1</sup> ) <sup>b</sup>
UDPNAG and FF to wild-type MurA (1UAE/1NAW) <sup>c</sup>	-2010	-810	-1200	-1.3
FPEP to wild-type MurA (1A2N/1NAW) <sup>c</sup>	-1760	-650	-1110	-1.32
FPEP to C115S mutant MurA (1A2N/1DLG) <sup>c</sup>	-2310	-1000	-1310	-1.3

<sup>a</sup> Accessible surface areas were calculated by subtraction of the surface of the free ligands and the free protein in the open conformation from the surface of the liganded protein in the closed conformation.

<sup>b</sup> Heat capacity changes were calculated on the basis of the values reported in ref 19. <sup>c</sup> Average values of chains a and b were taken for 1NAW and 1DLG (see Table 2).

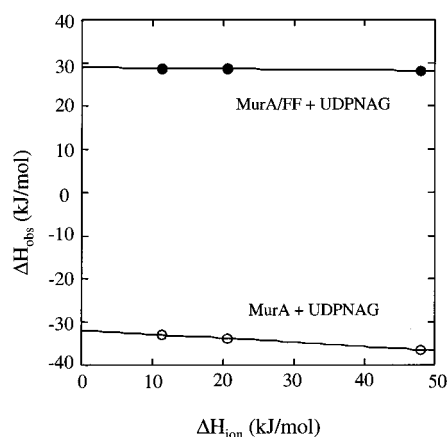


FIGURE 4: Protonation effect accompanying UDPNAG binding to free MurA and MurA–fosfomycin. Experimentally observed enthalpy changes,  $\Delta H_{\text{obs}}$ , were plotted as a function of the ionization enthalpy of the buffer,  $\Delta H_{\text{ion}}$ , at 15 °C to evaluate the protonation effect. The ITC experiments were performed in 50 mM PIPES, HEPES, and Tris, pH 7.4, containing 2 mM DTT and 0.5 mM EDTA. Open circles represent the experimental values for titrations of MurA with UDPNAG; solid circles represent the experimental values for titrations of the binary complex of MurA and fosfomycin with UDPNAG.

their  $pK_a$  values. Therefore, substrate binding can be accompanied by an exchange of protons between ionizable groups of amino acid residues and the buffer. As this contributes to the apparent enthalpy change,  $\Delta H_{\text{obs}}$ , measured in ITC, the observed enthalpies have to be corrected for the ionization enthalpy of the buffer by measuring the same process in buffers with different ionization enthalpies ( $\Delta H_{\text{ion}}$ ). The binding enthalpy can then be calculated according to

$$\Delta H_{\text{obs}} = \Delta H_{\text{bind}} + n_{\text{H}^+} \Delta H_{\text{ion}} \quad (2)$$

where  $n_{\text{H}^+}$  designates the number of protons that are released ( $n_{\text{H}^+} > 0$ ) or taken up ( $n_{\text{H}^+} < 0$ ) by the buffer (19). The enthalpies determined in 50 mM PIPES, HEPES, and Tris buffer, pH 7.4, for the binding of UDPNAG to MurA in the absence and presence of fosfomycin are summarized in Figure 4. As both processes are not a function of the buffer ionization enthalpy, the enthalpies observed in the ITC experiments do not require correction.

The measurements were also carried out in phosphate buffer, but as this seems to influence the thermodynamic parameters significantly, these data were not included in the

analysis. This could be due to phosphate binding in or near the binding site of UDPNAG or fosfomycin.

## DISCUSSION

The thermodynamic investigations presented here show that the binding of UDPNAG to free MurA is enthalpically driven with  $\Delta H = -35.5$  kJ mol<sup>-1</sup> at 15 °C (Scheme 2). The associated large negative entropy ( $-25$  J mol<sup>-1</sup> K<sup>-1</sup>) has been interpreted in terms of a conformational change (13). These changes in enthalpy and entropy for the binding of UDPNAG to free MurA could be explained as follows: the binding of UDPNAG to free MurA is dominated by contributions from van der Waals and/or hydrogen-bonding interactions (21). This is confirmed by structural data as the structure of MurA cocrystallized with UDPNAG and fosfomycin reveals a hydrophobic binding pocket for the nucleobase uridine and eight hydrogen bonds between UDPNAG and MurA (7). The formation of the hydrogen bonds is associated with a loss of motional freedom of the amino acid side chains involved in these interactions, which leads to a decrease in entropy. In contrast, the binding of UDPNAG to MurA–fosfomycin is an endothermic and entropically driven process. The favorable entropy could result from the release of water molecules from the active site into bulk solvent (19). A comparison of free MurA with the ternary complex (MurA, UDPNAG, fosfomycin) reveals that 13 water molecules are released from the active site upon ligand binding (22), not to mention the rearrangement of the solvent on the surface upon the conformational change. In addition, the observed heat absorption and the large positive entropy changes for the binding of UDPNAG to MurA–fosfomycin could result predominantly from hydrophobic interactions and desolvation of the substrate as well as the enzyme (21). A more comprehensive discussion of these differences in the thermodynamic parameters in the absence and presence of fosfomycin requires the availability of structural information of the binary complex of MurA with UDPNAG and fosfomycin, respectively. Both binding processes show an enthalpy/entropy compensation, which is described in the literature as an ubiquitous phenomenon for association reactions and is due to the properties of water as the solvent (23).

Previously reported binding studies suggested a partial conformational change upon UDPNAG binding to MurA (10). In particular, the effect of UDPNAG on the binding of the second substrate PEP and the ability to form the *O*-phosphothioketal reaction intermediate have been discussed in terms of a conformational change (13). UDPNAG exerts a similar effect on the binding of fosfomycin to MurA (9, 20). In a recent report, ITC experiments have supported the notion that fosfomycin binds preferentially in the presence of UDPNAG (13). Here, we have shown that fosfomycin binds covalently to C115 of MurA even in the absence of UDPNAG. Despite the synergistic effect on the binding of fosfomycin, the affinity of MurA for UDPNAG does not depend on the presence of fosfomycin ( $K_D$  in the absence of fosfomycin 25  $\mu\text{M}$ , in its presence 29  $\mu\text{M}$ ). Similarly, calorimetric studies of EPSP synthase from *E. coli* revealed a strong synergistic effect (80 000-fold) of S3P on the binding of the inhibitor glyphosate (24) but not vice versa. This is contradictory to thermodynamic studies reported recently for

binding of S3P and glyphosate to EPSP synthase of *Streptococcus pneumoniae* (25). The authors could determine a synergistic effect (1600-fold) for both ligands. This synergistic effect of S3P was interpreted in both cases as evidence for a conformational change upon S3P binding, resulting in a high-affinity binding site for glyphosate.

In agreement with the predicted conformational change, the thermodynamic characterization of the binding of UDPNAG to free MurA and MurA–fosfomycin revealed a large negative change in heat capacity. The experimentally determined heat capacities are  $-1.87$  and  $-2.74$   $\text{kJ mol}^{-1} \text{K}^{-1}$ , respectively. It is a common phenomenon that ligand binding is accompanied with negative changes in heat capacity, and the largest contribution is thought to be due to changes in solvent-accessible surface area (19). Calculation of the expected heat capacity change for the conformational change of free MurA (open conformation; see Figure 1, left structure) to the ternary complex (closed conformation; see Figure 1, right structure) resulted in  $\Delta C_p = -1.3$   $\text{kJ mol}^{-1} \text{K}^{-1}$ . This calculated heat capacity change for the whole process, including not only dehydration of the binding site but changes in hydration due to the conformational changes of the protein as well, is smaller than the experimentally measured  $\Delta C_p$  values for the individual steps (see Scheme 2). Therefore, the change in buried surface area is not the only process responsible for the changes in heat capacity. In principle, one can envisage additional sources of heat capacity changes upon ligand binding to a receptor site. Possible contributions from temperature-dependent conformational equilibria of free MurA itself (partial refolding upon binding) are unlikely since no changes of the CD signal were observed over the temperature range studied ( $15$ – $30$   $^{\circ}\text{C}$ ). Moreover, a comparison of the structures of free MurA (5) and the ternary complex (7) demonstrates that binding is not associated with any changes in secondary structure. It is possible that conformational changes associated with temperature-dependent enthalpic processes contribute to the heat capacity change. These may involve newly formed interactions upon conformational change such as the movement of the loop comprising residues 112–121, which then forms multiple interactions with the ligands and protein groups in the vicinity of the binding pocket.

It has been argued that heat capacity is a measure of the width of the distribution of enthalpic microstates (21). Ligands bind preferentially to certain microstates, which results in a shift of the average enthalpy and in a restriction to less possible microstates. If the ligand binding shifts a preexisting equilibrium between “binding-competent” (A) and “binding-incompetent” (B) receptor conformations, an additional contribution to the heat capacity will result (26, 27). It arises from the thermodynamic coupling of binding to the equilibrium  $A \leftrightarrow B$  and is not zero even if the heat capacity characterizing the  $A \leftrightarrow B$  transition is negligibly small. In the case of MurA, this can be rationalized as follows. The unliganded MurA in its open conformation is flexible, which allows the domains and the loop to move. UDPNAG binds preferentially to a less flexible form that is closer to the closed crystallographic conformation with the two domains tightly packed and the loop fixed in the active site (7) (see also Figure 5). One important prediction of the “conformational selection” model is that  $\Delta H$  vs  $T$  plots will not be linear, thus reflecting temperature dependence of the

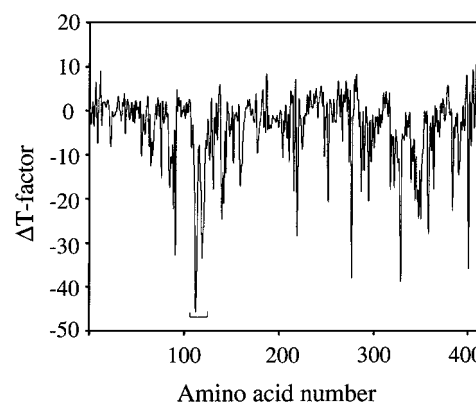


FIGURE 5: Influence of UDPNAG and fosfomycin binding on the temperature factors observed for MurA. From the temperature factors of each atom as reported in the corresponding PDB file the average temperature factor of each amino acid in the open (1NAW) and closed (1UAE) conformations was calculated. Here the difference of the temperature factor of each amino acid in the open and closed conformations is plotted against the amino acid number. The catalytic loop comprising amino acids 112–121 is marked.

heat capacity. However, in our hands, the apparent experimental heat capacity decrements for the two reactions studied do not display any statistically significant temperature dependence between  $15$  and  $30$   $^{\circ}\text{C}$  (Figure 3). Two explanations are possible. Either the temperature interval of the experiments is too narrow to detect a nonlinear dependence of  $\Delta H$  on  $T$  or, else, the conformational selection model does not apply in the case of MurA.

A comparison of the two experimentally determined  $\Delta C_p$  changes reveals that ca. 70% of the heat capacity change is associated with the binding of UDPNAG to free MurA relative to the binding of UDPNAG to form the ternary complex (see Scheme 2). Since  $\Delta C_p = -1.87$   $\text{kJ mol}^{-1} \text{K}^{-1}$  for the binary MurA–UDPNAG complex exceeds the calculated  $\Delta C_p = -1.3$   $\text{kJ mol}^{-1} \text{K}^{-1}$  for the whole process, most of the conformational change is associated with this step. We propose that the additional change in heat capacity measured for the formation of the ternary complex of MurA–UDPNAG–fosfomycin is caused by loss of vibrational modes in the ternary complex. “Soft” internal degrees of freedom with fundamental frequencies less than  $500$ – $800$   $\text{cm}^{-1}$  are assumed to be important contributions in binding and conformational transitions involving proteins (28). Tidor and Karplus demonstrated by computational methods that many modes below  $400$ – $600$   $\text{cm}^{-1}$  contribute to the vibrational entropy and heat capacity of protein–protein and protein–ligand binding (29). In another recent theoretical study, frequencies below  $200$   $\text{cm}^{-1}$  have been identified as the fundamental source of vibrational contributions to the thermodynamics of conformational changes in proteins (30). Furthermore, vibrational contributions are not restricted to the protein. The reduction of translational and soft vibrational modes of bound water is thought to have a pronounced effect on the thermodynamics of ligand binding (28, 31). As already mentioned, there is sound crystallographic evidence that water participates in one way or another in ligand binding to MurA. The importance of vibrational effects to the thermodynamics of formation of the ternary complex is supported with results obtained by limited proteolysis (11). One strong indication of the restriction of soft vibrational modes is the change of temperature ( $B$ ) factors. As shown

in Figure 5, the closed conformation has overall lower temperature factors compared to the open conformation. Notably, the most prominent decrease in temperature factors is observed for residues 112–121 which are located in the loop that forms multiple interactions with residues in the active site and the ligands. Taken together, the thermodynamic, structural, and biochemical information available so far strongly indicates that the presence of fosfomycin in the ternary MurA–UDPNAG–fosfomycin complex leads to a reduction of the vibrational content of the enzyme.

## ACKNOWLEDGMENT

We thank Dr. Teresa Fitzpatrick and Alison Thomas for critically reading the manuscript.

## REFERENCES

- Bugg, T. D. H., and Walsh, C. T. (1992) *Nat. Prod. Rep.*, 199–215.
- Roberts, F., Roberts, C. W., Johnson, J. J., Kyle, D. E., Krell, T., and Coggins, J. R. (1998) *Nature* 393, 801–805.
- Schmid, J., and Amrhein, N. (1999) in *Plant Amino Acids: Biochemistry and Biotechnology* (Singh, B. K., Ed.) pp 147–169, Marcel Dekker, New York.
- Lauer, B., Süßmuth, R., Kaiser, D., Jung, G., and Bormann, C. (2000) *J. Antibiot.* 53, 385–392.
- Schönbrunn, E., Sack, S., Eschenburg, S., Perrakis, A., Krekel, F., Amrhein, N., and Mandelkow, E. (1996) *Structure* 4, 1065–1075.
- Stallings, W. C., Abdel-Meguid, S. S., Lim, L. W., Shieh, H.-S., Dayringer, H. E., Leimgruber, N. K., Stegeman, R. A., Anderson, K. S., Sikorski, J. A., Padgett, S. R., and Kishore, G. M. (1991) *Proc. Natl. Acad. Sci. U.S.A.* 88, 5046–5050.
- Skarzynski, T., Mistry, A., Wonacott, A., Hutchinson, S. E., Kelly, V. A., and Duncan, K. (1996) *Structure* 4, 1465–1474.
- Skarzynski, T., Kim, D. H., Lees, W. J., Walsh, C. T., and Duncan, K. (1998) *Biochemistry* 37, 2572–2577.
- Schönbrunn, E., Eschenburg, S., Krekel, F., Luger, K., and Amrhein, N. (2000) *Biochemistry* 39, 2164–2173.
- Schönbrunn, E., Svergun, D. I., Amrhein, N., and Koch, M. H. J. (1998) *Eur. J. Biochem.* 253, 406–412.
- Krekel, F., Oecking, C., Amrhein, N., and Macheroux, P. (1999) *Biochemistry* 38, 8864–8878.
- Wanke, C., and Amrhein, N. (1993) *Eur. J. Biochem.* 218, 861–870.
- Samland, A. K., Amrhein, N., and Macheroux, P. (1999) *Biochemistry* 38, 13162–13169.
- Fukada, H., and Takahashi, K. (1998) *Proteins: Struct., Funct., Genet.* 33, 159–166.
- Perozzo, R., Jelesarov, I., Bosshard, H. R., Folkers, G., and Scapozza, L. (2000) *J. Biol. Chem.* 275, 16139–16145.
- Samland, A. K., Etezady-Esfarjani, T., Amrhein, N., and Macheroux, P. (2001) *Biochemistry* 40, 1550–1559.
- Krekel, F., Samland, A. K., Macheroux, P., Amrhein, N., and Evans, J. N. S. (2000) *Biochemistry* 39, 12671–12677.
- Hubbard, S. J., and Thornton, J. M. (1996) *NACCESS Computer Program, Version 2.1.1*, Department of Biochemistry and Molecular Biology, University College, London.
- Baker, B. M., and Murphy, K. P. (1998) *Methods Enzymol.* 295, 294–315.
- Marquardt, J. L., Brown, E. D., Lane, W. S., Haley, T. M., Ichikawa, Y., Wong, C.-H., and Walsh, C. T. (1994) *Biochemistry* 33, 10646–10651.
- Eftink, M., and Biltonen, R. (1980) Thermodynamics of interacting biological systems, in *Biological Microcalorimetry*, pp 343–412, Academic Press, New York.
- Eschenburg, S., and Schönbrunn, E. (2000) *Proteins* 40, 290–298.
- Lumry, R., and Rajender, S. (1970) *Biopolymers* 9, 1125–1227.
- Ream, J. E., Yuen, H. K., Frazier, R. B., and Sikorski, J. A. (1992) *Biochemistry* 31, 5528–5534.
- Du, W., Liu, W.-S., Payne, D. J., and Doyle, M. L. (2000) *Biochemistry* 39, 10140–10146.
- Bruzzese, F. J., and Connelly, P. R. (1997) *Biochemistry* 36, 10428–10438.
- Ferrari, M. E., and Lohman, T. M. (1994) *Biochemistry* 33, 12896–12910.
- Sturtevant, J. (1977) *Proc. Natl. Acad. Sci. U.S.A.* 74, 2236–2240.
- Tidor, B., and Karplus, M. (1994) *J. Mol. Biol.* 238, 405–414.
- Ma, B., Tsai, C.-J., and Nussinov, R. (2000) *Biophys. J.* 79, 2739–2753.
- Morton, J. G., and Ladbury, J. E. (1996) *Protein Sci.* 5, 2115–2118.

BI0107041